마이크로 콜드 가스 추력기의 선행 연구

문성환* · 오화영* · 허환일**

Preliminary Study of Micro Cold Gas Thruster

Seonghwan Moon* · Hwayoung Oh* · Hwanil Huh**

ABSTRACT

Miniaturization of subsystems including propulsion systems is recent trends in spacecraft technology. Small space vehicle propulsion is not only a technological challenge of a scaling system down, but also a combination of fundamental flow/combustion constraints. In this paper, physical constraints of micronozzle for cold gas micro-thruster are reviewed and discussed. Method to measure small thrust are also described.

초 록

추진 시스템을 포함해 구성요소의 소형화가 최근 위성체 기술의 경향이다. 소형위성 추진기관은 크기 축소라는 기술적 도전일 뿐만 아니라, 기본적인 유동/연소 구속조건의 결합을 보이고 있다. 본 논문에서는 냉각 가스 마이크로 추력기에서 마이크로 노즐의 물리적 구속조건에 대해 살펴보았다. 또한 미소 추력의 측정 방법에 대해서도 언급하였다.

Key Words: Micro Propulsion(마이크로 추진), Thrust Measurement(추력 측정)

1. Introduction

In recent years, there has been interest toward the reducing the size of spacecraft, so that the cost and risk of missions can be reduced. With the miniaturization of spacecraft, micropropulsion modules are

† 2004년 3월 15일 접수 ~ 2004년 5월 11일 심사완료
* 학생회원, 충남대학교 대학원 항공우주공학과
** 종신회원, 충남대학교 항공우주공학과
연락저자, E-mail: hwanil@cnu.ac.kr

required to produce very small (below the Newton) and highly accurate forces for stabilization, pointing, and station keeping of microsatellite. There is a point where reduced-scale versions of conventional propulsion systems will no longer be practical. This restriction is not only a result of practical volume, mass and power limitations, but also of the physics at reduced scale, where forces ignored at conventional scale become dominant. At this point, a fundamentally different approach to propulsion must be taken.

Micropropulsion systems not only have to be reduced scale in mass and volume, but also use little or no power, be relatively simple yet flexible enough to use in multifunctions, and be cost effective for what is likely to be a relatively low-cost spacecraft.

In an attempt to standardize the definition of microspacecraft, the Air Force Research Laboratory(AFRL) has proposed the standard detailed in Table 1.

Table 1. Small satellite classification standard[1]

Total spacecraft mass	Description
100-1000 kg	Small satellite
10-100 kg	Micro satellite
1-10 kg	Nano satellite
0.1-1 kg	Pico satellite
10-100 g	Femto satellite
1-10 g	Atto satellite
0.1-1 g	Zepto satellite

Among the propulsion systems frequently used in spacecraft, chemical systems have the lowest complexity and cost. They can provide highly repeatable, extremely small impulse bit (Ibit) for accurate orbit maintenance and attitude control.

The micronozzle is an essential component of many propulsion systems, and its success will lead the way for more advanced chemical systems. Thus, with many of the technologies currently under investigation, the micronozzle, which is the heart of the cold gas system, is chosen as the focus of research. And, in order to test such micronozzle, we design the thrust measurement system for small thrust level.

2. Scaling Issue

There are several system performance drivers that lead to the selection of smaller scale components. In most case, these are driven by the "square" law[2]. In other words, properties of a function of the area of interaction decrease more slowly than those of a function of volume. This is formulated as

$$\frac{f(area)}{f(volume)} \propto \frac{L^2}{L^3} \propto \frac{1}{L} \tag{1}$$

Thus, as the length scale (L) is reduced the property ratio increases.

An example is the thrust-to-mass ratio of a spacecraft. This determines the effectiveness of the system as an actuator. When considering the engine, which includes the nozzle and chamber, the thrust-to-mass ratio can be formulated as

$$\frac{F_t}{m_{eng}} \propto \frac{P_c L^2}{P_c L^3} \propto \frac{1}{L} \tag{2}$$

where Pc is the chamber pressure, and L is a characteristic dimension, such as the throat diameter.

However, the dominant mass comes from the propellant and the tank for cold-gas propulsion system. Thus, a reduction in scale does not significantly increase the thrust-to-mass ratio of the entire propulsion system as long as the tank pressure and propellant mass remains constant.

If the Isp increases, the amount of propellant required for a given mission decreases, and a reduction of system mass occurs. If the nozzle scale is reduced, lower thrust is achieved. By reducing the scale, higher chamber pressure can be used to achieve the same low thrust.

However, when scale is getting smaller, nozzle suffers high viscous losses due to the low Reynolds number. For the circular nozzle, frictional losses are governed by Reynolds number which is defined as

$$R_e = \frac{\rho_t u_t D_t}{\mu_t} = \frac{4\dot{m}}{\mu\pi D_t} \tag{3}$$

where ρ is the chamber density (proportional to chamber pressure), u is the velocity, D is the throat diameter, and μ is the viscosity, all at the defined throat condition.

In order to reduce viscous losses the Reynolds number may be increased by increasing chamber pressure. The thrust can be expressed in terms of the Reynolds number as

$$F \propto \dot{m} u_e = \frac{1}{4} R_e \mu D \pi u_e \tag{4}$$

Thus, assuming F and u_e stay constant, the corresponding reduction of nozzle of characteristic nozzle throat size is required to compensate for the increase in the flow Reynolds number in order to maintain the same thrust. This results in lower frictional losses, and a higher delivered Isp. Though the tank mass will not directly reduce with scale, the amount of propellant required is less due to the higher Isp, and the engine mass is also less. Thus the thrust to propulsion system mass can be increased significantly with a reduction in scale.

Boundary layer growth is a function of the nozzle length, or divergence angle for a given expansion. As divergence angle increases, boundary layer thickness decreases, which decreases blockage and increases performance. However, large divergence angles increase the momentum component perpendicular to the thrust axis, which is lost as useful thrust.

In general, the performance of circular cross-sectional nozzles is higher than the non-circular ones. This is due to higher friction and heat transfer losses for non-circualr nozzles. Zakirov explains the reasons as follows[3]. Formation of boundary layer at the flat end wall leads to higher friction losses since increases in boundary-layer thickness is not compensated by flow channel expansion in that direction. For non-circular nozzle, cross-sectional perimeter -to-area ratio is always higher than that of for circular one. For the same hydraulic area, however, high aspect ratios for 2-D, rectangular nozzle suggest that the width dimension must be much smaller than circular nozzle diameter. Therefore, this dimension will be responsible for lower nozzle flow Reynolds number, and thus for higher friction losses due to the development of thicker boundary layer.

The nature of the MEMS manufacturing process results in rectangular rather than circular nozzle. Therefore, we decide to adopt the micro milling technique for machining circular nozzle.

3. Design of Cold Gas Microthruster

The cold gas thruster is a much simple piece of hardware than other propulsion systems. It is a well understood device and its performance is therefore limited almost exclusively by the inherent propellant properties and scaling issues. The two main components of the cold gas thruster are the nozzle and the valve.

The thrust is determined by Newton's second law of motion under the assumption of constant gas property. Thrust is

$$F = \dot{m} c \tag{5}$$

Using the definition of thrust coefficient, thrust can be expressed as

$$F = \lambda C_F P_c A_t \tag{6}$$

$$\lambda = \frac{1+\cos\alpha}{2} \tag{7}$$

$$C_F = \sqrt{\frac{2\gamma^2}{\gamma-1}\left(\frac{2}{\gamma+1}\right)^{\frac{\gamma+1}{\gamma-1}}\left[1-\left(\frac{P_e}{P_C}\right)^{\frac{\gamma-1}{\gamma}}\right]} \tag{8}$$

Thruster chamber pressure can be varied from 2 to 20 bar. To investigate effects of scaling down, we change the nozzle throat diameter: 2.0, 1.0, 0.5, and 0.25 mm. Predicted thrusts are presented in Table 2. And mechanical design of cold gas thruster is given in Fig. 1.

One of the main drawback of these simple thrusters is their very low specific impulse, which generally ranges from about 40 to 65 seconds[4]. (except for helium, which is approximately 150 seconds.)

Table 2. Predicted thrust (gas: N2)

Nozzle throat diameter [mm]	Pc [bar]		
	2.0	10.0	20.0
	Thrust [N]		
0.25	0.0075	0.0615	0.1343
0.5	0.03	0.246	0.5374
1.0	0.1201	0.9839	2.1494
2.0	0.4805	3.9357	8.5976

4. Thrust Measurement Method

Measuring a force of the order of the Newton is common and many commercially available force sensors can be used.

Table 3. Mechanical methods of low-thrust measurement

Measured	Balancing force	Structure	Advantage	Problem
Momentum flux of exhaust plume	gravity(exerted on target)	target	simple	change of exhaust plume
Reaction force	elastic force	elastic member	quick response	thermal effects, Vibration
Reaction force	gravity	balance	without nonlinear relation (no deflection), small thermal effect	friction at fulcrum, slow response
Reaction force	gravity	pendulum	small thermal effect	friction at fulcrum, slow response

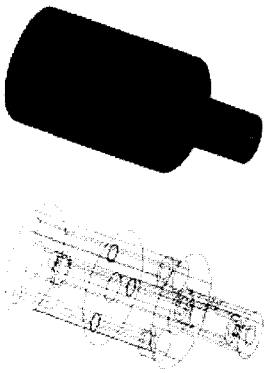

Fig. 1 Cold gas thruster design

However, when the thrust level decreases to milli-Newton, specific methods and equipments are needed to detect it accurately.

The ideal thrust measurement systems have an infinite stiffness. However, the difficulty when designing low thrust and dynamic measurement system is the dilemma met between sensitivity and band width[5]. To obtain a high natural frequency system, one must stiffen the mechanical part that cause a decrease in thrust measurement sensitivity.

The mechanical methods of low thrust measurements are categorized in Table 3[6]. Among these methods, we adopt the strain gauge based thrust measurement system. Strain gauge sensor has been employed because of its simplicity, cost effectiveness, response[7]. However, the deflection-thrust relation is affected by the temperature of the elastic member. Also, the thrust signal can be easily disturbed even by small facility induced vibration. So natural frequency is measured and then its bandwidth is eliminated for measuring thrust by low pass filter. A test result of natural frequency is shown in Fig. 2. Signal conditioning circuity which includes the low pass filter is shown in Fig. 3. Here, natural frequency is approximately 113Hz. And cutoff frequency is determined by R9, R11, C3, C4, R17, R19, C7 and C49.

The thrust measurement system is shown in Fig. 4. It consists of plates, four columns and eight bars. The bottom plate is fixed and the upper plate moves in response to a thrust.

When the thrust measurement system is critically loaded, four columns produce a large deflection even a small thrust in the transverse direction. And these deflection are directly proportional to the thrust.

The buckling load P is determined using the Euler equation.

$$P = 4\pi^2 EI/L^2 \tag{9}$$

where E is the Young's modulus of the column,

I is the moment of inertia and L is the length of the column.

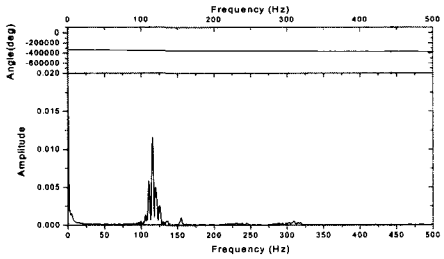

a) FFT graph

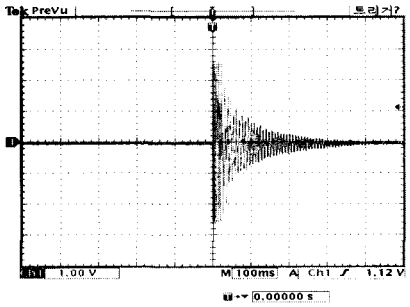

b) Oscilloscope graph

Fig. 2 Natural frequency of thrust measurement system

Before the columns are critically loaded, additional weights in the form of plates are attached to the upper plate.

Each column of the thrust measurement system has four active arms(strain gauge). This arrangement provides excellent temperature compensation and linearity. Two gauges which tensile strain form one pair of opposite arms of the Wheatstone bridge and the other two strain gauges which undergo compressive strain form the other pair of opposite arms of the bridge. This produces the maximum differential voltage.

In order to calibrate the output voltage from the thrust measurement system, we gradually increase the load. Some calibration results are shown in Fig. 5 showing a good linearity. We plot each loop gain in Fig. 6. According to this curve, we can choose the appropriate load. For example, if we choose the load 4000 g, loop gain is 40 mV/g. If one choose the heavier load, loop gain will be larger.

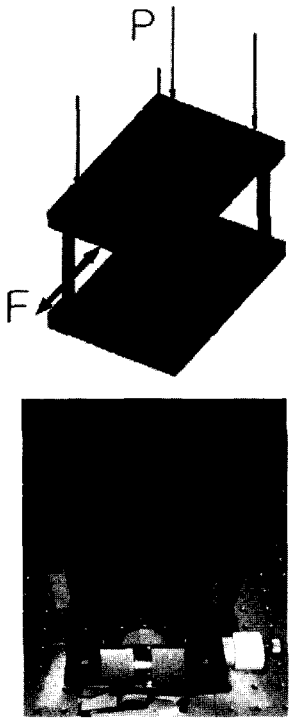

Fig. 4 A schematic diagram of proposed thrust measurement system

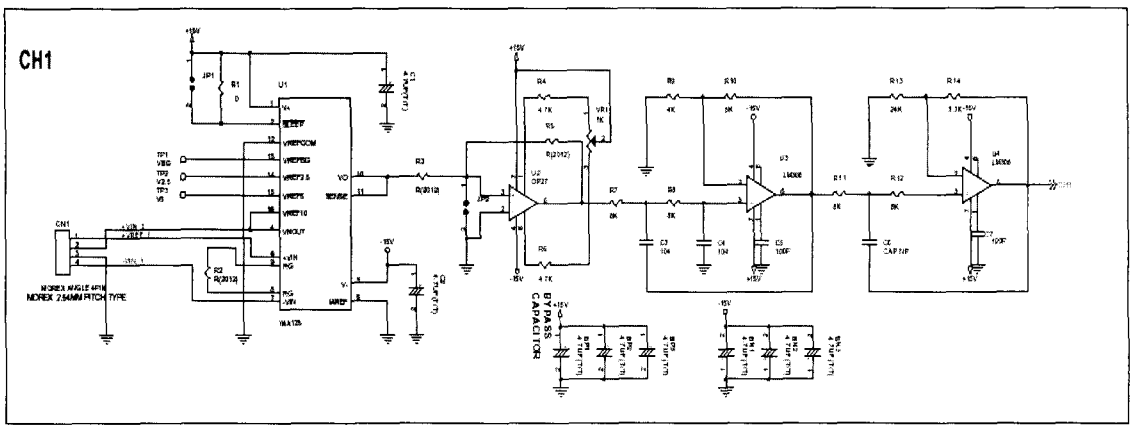

Fig. 3 Signal conditioning and low pass filter circuitry

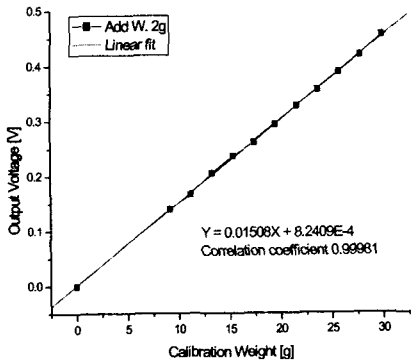

a) Load 765.02g

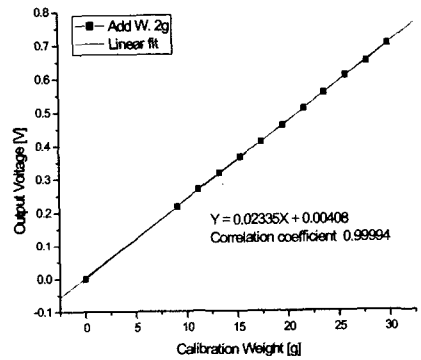

b) Load 2642.67g

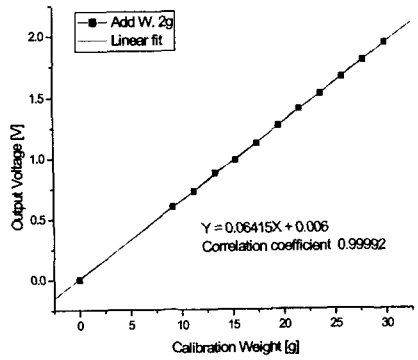

c) Load 4864.1g

Fig. 5 Linearity curve of thrust measurement system

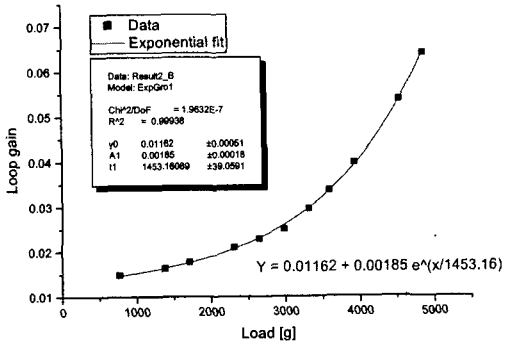

Fig. 6 Exponential curve of load vs loop gain

Acknowledgements

This work was partially supported by grant No. KOSEF R01-2003-000-11735-0(2003) from the basic research program of the Korea Science & Engineering Foundation.

Reference

1. Michael M. Micci and Andrew D. Ketsdever, Micropropulsion for small spacecraft, Progress in Aeronautics and Astronautics, Volume 187, AIAA, 2000
2. Robert L. Bayt.: Analysis, "Fabrication and testing of a MEMS-based Micropropulsion System," 1999, pp. 23-25
3. V. Zarkirov, D.Gibbon, and M. Sweeting, Bob Reinicke, Ray Bzibziak, and Timothy Lawrence, "Specifics of Small Satellite Propulsion Part 2," AIAA 2001-3834, 37th /ASME/SAE/ASEE Joint Propulsion Conference and Exhibit, 2001
4. Jeffrey G. Reichbach, Raymond J. Sedwick and Manuel Martinez-Sanchez, " Micropropulsion System Selection for Precision Formation Flying Satellites," SERC#1-01, January 2001, pp

84-85
5. S. Orieux, C. Rossi and D. Esteve, "Thrust stand for ground tests of solid propellant microthrusters," American Institute of Physics, Volume 73, Number 7, 2002
6. Akihiro Sasoh and Yoshihiro Arakawa, "A high-resolution thrust stand for ground tests of low-thrust space propulsion devices," American Institute of Physics, 1993, pp. 719-720
7. R. John Stephen, K Rajanna, Vivek Dhar, K G Kalyan Kumar and S Nagabushanam, "Strain gauge based thrust measurement system for a statioinary plasma thruster," IOP Publishing Ltd, UK, 2001, pp. 1568-15670